



Second-order Synchrosqueezing Transform: The Wavelet Case and Comparisons

Duong-Hung Pham, Sylvain Meignen

► To cite this version:

Duong-Hung Pham, Sylvain Meignen. Second-order Synchrosqueezing Transform: The Wavelet Case and Comparisons. 2017. hal-01586372v1

HAL Id: hal-01586372

<https://hal.science/hal-01586372v1>

Preprint submitted on 6 Sep 2017 (v1), last revised 30 May 2018 (v4)

HAL is a multi-disciplinary open access archive for the deposit and dissemination of scientific research documents, whether they are published or not. The documents may come from teaching and research institutions in France or abroad, or from public or private research centers.

L'archive ouverte pluridisciplinaire **HAL**, est destinée au dépôt et à la diffusion de documents scientifiques de niveau recherche, publiés ou non, émanant des établissements d'enseignement et de recherche français ou étrangers, des laboratoires publics ou privés.

Second-order Synchrosqueezing Transform: The Wavelet Case and Comparisons

Duong-Hung Pham¹, and Sylvain Meignen²
^{1,2}Jean Kuntzmann Laboratory- Bâtiment IMAG,
Université Grenoble Alpes
700 Avenue Centrale
Campus de Saint Martin d'Hères
38401 Domaine Universitaire de Saint-Martin-d'Hères.

Abstract

This paper addresses the analysis of the time-frequency technique so-called the second-order synchrosqueezing transform derived from continuous wavelet transform of multicomponent AM-FM signals. Such a technique is designed to deal with the signals consisting of strong frequency modulation components or modes. Before going into the details of this analysis, we revisit the case where the modes are assumed to be with weak frequency modulation as in the seminal paper of Daubechies et *al.* [1], but not assuming the wavelet is compactly supported in the Fourier domain. The remainder of the paper is devoted to the theoretical analysis of the second order wavelet-based synchrosqueezing transform [2] and we then put forward its differences compared with variants of the proposed technique. Numerical simulations assessing and comparing the quality of the different synchrosqueezing operators conclude the paper.

Keywords: Time-frequency analysis, reassignment, synchrosqueezing, AM/FM, multicomponent signals.

¹Email:duong-hung.pham@imag.fr

²Email:sylvain.meignen@imag.fr

1. Introduction

Many signals arising from audio recordings (music, speech), meteorology, structural stability analysis [3, 4, 5], or medical data (electrocardiogram, thoracic and abdominal movement signals) [6, 7], can be modeled as a sum of amplitude- and frequency-modulated (AM-FM) modes, called multicomponent signals (MCS) [8]. Time-frequency (TF) analysis plays a central role for characterizing such signals and, in that framework, numerous methods have been developed for the last two decades. Standard linear methods, as for instance the short-time Fourier transform (STFT) and the continuous wavelet transforms (CWT), have been the most commonly used [9]. However, the effectiveness of each method strongly depends on the nature of the modes constituting the signal and is limited by the trade-off between time and frequency resolution known as *uncertainty principle*. Several attempts were made to overcome this shortcoming and one of them, called the *reassignment method* (RM), received a considerable attention. The concept of RM dates back to Koderer et al. [10] in the 1970's and was further developed in [11], where it was viewed as a means of improving the readability of TF representations. Unfortunately, RM suffers from an inherent limitation which is its non invertibility, namely it does not allow for mode reconstruction.

In an independent work [1], Daubechies et al. introduced an adaptive wavelet-based signal analysis method known as the *synchrosqueezing transform* (WSST), an adaptation of RM enabling modes' retrieval. An extension of WSST to the TF representation given by STFT was proposed in [12], while many other efforts were also devoted to explore the bidimensional case, as for instance by using the monogenic synchrosqueezed wavelet transform [13], other types of TF representations as the synchrosqueezed wavelet packet transform [14, 15], or multi-taper approaches as in the ConceFT technique [16]. In spite of all these advances, one major problem associated with synchrosqueezing techniques in their original formulation is that they cannot deal with MCS containing modes with strong frequency modulation, very common in many fields of practical interest, as for instance chirps involved in radar [17], speech processing [18], or gravitational waves [19, 20]. In this regard, an adaptation of FSST to better handle that type of signals, known as the *second order synchrosqueezing transform* (FSST2), was introduced in [21] and its theoretical foundations settled in [22].

In the present paper, our goal is to extend FSST2 to the wavelet case.

To do so, after having recalled some useful definitions in Section 2, we revisit WSST assuming the analysis wavelet is not compactly supported in the Fourier domain, in Section 3. This helps derive, in Section 4, the second order wavelet-based synchrosqueezing transform (WSST2) and then prove approximations results generalizing those related to WSST. In Section 5, we then introduce variants of WSST2 which we finally compare with the latter, both in terms of the quality of TF representation and mode reconstruction, in Section 6.

2. Background

Before going in detail into the principle of WSST, the following section presents several useful notation and definitions.

2.1. Fourier transform

The Fourier transform (FT) of a given signal $f \in L^1(\mathbb{R})$ is defined as:

$$\hat{f}(\eta) = \mathcal{F}\{f\}(\eta) = \int_{\mathbb{R}} f(t) e^{-i2\pi\eta t} dt. \quad (1)$$

If \hat{f} is also integrable, f can be reconstructed through:

$$f(t) = \int_{\mathbb{R}} \hat{f}(\eta) e^{i2\pi\eta t} d\eta. \quad (2)$$

2.2. Continuous wavelet transform

Let us consider $\psi \in L^1(\mathbb{R})$ and $f \in L^\infty(\mathbb{R})$, and then define for any time t and scale $a > 0$, the *continuous wavelet transform* (CWT) of f by:

$$W_f^\psi(t, a) = \frac{1}{a} \int_{\mathbb{R}} f(\tau) \psi\left(\frac{\tau - t}{a}\right)^* d\tau. \quad (3)$$

2.3. Multicomponent signal

In this paper, we will intensively study multicomponent signals (MCS) defined as a superposition of AM-FM components or modes:

$$f(t) = \sum_{k=1}^K f_k(t) \quad \text{with} \quad f_k(t) = A_k(t) e^{i2\pi\phi_k(t)}, \quad (4)$$

for some finite $K \in \mathbb{N}$, $A_k(t)$ and $\phi'_k(t)$ are respectively instantaneous amplitude (IA) and frequency (IF) of mode f_k satisfying: $A_k(t) > 0$, $\phi'_k(t) > 0$ and $\phi'_{k+1}(t) > \phi'_k(t)$ for all t . Such a signal is fully described by its ideal TF (ITF) representation defined as:

$$\text{TI}_f(t, \omega) = \sum_{k=1}^K A_k(t) \delta(\omega - \phi'_k(t)), \quad (5)$$

where δ denotes the Dirac distribution.

3. Wavelet-based synchrosqueezing transform (WSST)

3.1. WSST principle

The wavelet-based SST (WSST) was originally introduced in the context of auditory signal analysis [23] and further studied mathematically in [1]. Its principle is to sharpen the “blurred” representation given by the CWT by using the following IF estimate at time t and scale a :

$$\hat{\omega}_{W_f^\psi}(t, a) = \Re \left\{ \frac{1}{i2\pi} \frac{\partial_t W_f^\psi(t, a)}{W_f^\psi(t, a)} \right\}, \quad (6)$$

where $\Re\{Z\}$ stands for the real part of complex number Z and ∂_t is the partial derivative with respect to t .

Indeed, $W_f^\psi(t, a)$ is reassigned to a new position $(t, \hat{\omega}_{W_f^\psi}(t, a))$ using the synchrosqueezing operator defining WSST, as follows:

$$S_{W_f^\psi}^{\gamma, \alpha}(t, \omega) = \frac{1}{C'_\psi} \int_{\mathbb{A}(\gamma, \alpha)} W_f^\psi(t, a) \delta(\omega - \hat{\omega}_{W_f^\psi}(t, a)) \frac{da}{a}, \quad (7)$$

where $\mathbb{A}(\gamma, \alpha) = \{a \in [0, \alpha] \text{ s.t. } |W_f^\psi(t, a)| > \gamma\}$, with γ some threshold, α being defined later in the paper, and $C'_\psi = \int_0^{+\infty} \hat{\psi}^*(\eta) \frac{d\eta}{\eta} < \infty$.

Since the coefficients of CWT are reassigned along the “scale” axis, WSST preserves the causality property, thus making the k^{th} mode approximately reconstructed by integrating $S_{W_f^\psi}^{\gamma, \alpha}(t, \omega)$ in the vicinity of the corresponding ridge $(t, \frac{1}{\phi'_k(t)})$ in the time-scale (TS) plane:

$$f_k(t) \approx \int_{\{\omega, |\omega - \phi'_k(t)| < d\}} S_{W_f^\psi}^{\gamma, \alpha}(t, \omega) d\omega, \quad (8)$$

where $\varphi_k(t)$ is an estimate of $\phi'_k(t)$, which is often computed by a ridge extraction technique. Parameter d enables to compensate for both the inaccurate approximation $\varphi_k(t)$ of $\phi'_k(t)$ and the error made by estimating the IF by means of $\hat{\omega}_{W_f^\psi}(t, a)$.

3.2. WSST mathematical framework

WSST is supported by a solid mathematical framework [1], which we now recall. Let us first define the class of chirp-like functions (signals) on which one builds the theory:

Definition 1. Let $\varepsilon > 0$ and $\Delta \in (0, 1)$. The set $\mathcal{A}_{\Delta, \varepsilon}$ of multicomponent signals with modulation ε and separation Δ corresponds to signals defined in (4) with f_k satisfying:

$$\begin{aligned} A_k &\in C^1(\mathbb{R}) \cap L^\infty(\mathbb{R}), \phi_k \in C^2(\mathbb{R}), \\ \inf_{t \in \mathbb{R}} \phi'_k(t) &> 0, \sup_{t \in \mathbb{R}} \phi'_k(t) < \infty, M = \max_k (\sup_{t \in \mathbb{R}} \phi'_k(t)), \\ A_k(t) &> 0, |A'_k(t)| \leq \varepsilon \phi'_k(t) \leq \varepsilon M, |\phi''_k(t)| \leq \varepsilon \phi'_k(t) \leq \varepsilon M, \quad \forall t \in \mathbb{R}. \end{aligned}$$

Further, the f_k s are separated with resolution Δ , i.e., for all $k \in \{1, \dots, K-1\}$ and all t

$$\phi'_{k+1}(t) - \phi'_k(t) \geq \Delta(\phi'_{k+1}(t) + \phi'_k(t)). \quad (9)$$

Definition 2. Let h be a positive L^1 -normalized window belonging to $C_c^\infty(\mathbb{R})$, define $\alpha = \frac{1+\Delta}{\inf_{t \in \mathbb{R}} \phi'_1(t)}$, and consider $\gamma, \lambda > 0$, the wavelet-based synchrosqueezing transform of f with threshold γ and accuracy λ is defined by:

$$S_{W_f^\psi}^{\lambda, \gamma, \alpha}(t, \omega) := \frac{1}{C_\psi'} \int_{\mathbb{A}(\gamma, \alpha)} W_f^\psi(t, a) \frac{1}{\lambda} h\left(\frac{\omega - \hat{\omega}_{W_f^\psi}(t, a)}{\lambda}\right) \frac{da}{a}. \quad (10)$$

If $\lambda \rightarrow 0$, then $S_{W_f^\psi}^{\lambda, \gamma, \alpha}(t, \omega)$ tends, in the sense of distribution, to some value which we formally write as in (7).

Remark 1. It is interesting to point out that parameter α did not appear in the initial formulation of [1], but we will explain later why it is necessary.

Theorem 1. Consider $f \in \mathcal{A}_{\Delta, \varepsilon}$, set $\tilde{\varepsilon} = \varepsilon^{\frac{1}{3}}$ and let ψ be a non-compactly supported wavelet in the Fourier domain but satisfying: $|\hat{\psi}(\tau)(\eta)| \leq N_0 \varepsilon$ when $|\eta - 1| > \Delta$, and $\int_{\{\eta \text{ s.t. } |\eta - 1| > \Delta\}} |\hat{\psi}(\tau)(\eta)| \frac{d\eta}{\eta} \leq N_1 \tilde{\varepsilon}$, for some constants N_0 and N_1 .

Assuming $(t, a) \in \mathbb{E} = \mathbb{R} \times [0, \alpha]$ with α introduced in Definition 2, then, provided ε is sufficiently small, the following hold:

- (a) $|W_f^\psi(t, a)| > \tilde{\varepsilon}$ only when, there exists $k \in \{1, \dots, K\}$, such that $(t, a) \in Z_k := \{(t, a), \text{ s.t. } |a\phi'_k(t) - 1| < \Delta\}$.
- (b) For each $k \in \{1, \dots, K\}$ and all $(t, a) \in Z_k$ for which holds $|W_f^\psi(t, a)| > \tilde{\varepsilon}$, one has:

$$|\hat{\omega}_{W_f^\psi}(t, a) - \phi'_k(t)| \leq \tilde{\varepsilon}. \quad (11)$$

- (c) Moreover, for each $k \in \{1, \dots, K\}$, there exists a constant $D_W^{[1]}$ such that for any $t \in \mathbb{R}$

$$\left| \lim_{\lambda \rightarrow 0} \left(\int_{|\omega - \phi'_k(t)| < \tilde{\varepsilon}} S_{W_f^\psi}^{\lambda, \tilde{\varepsilon}, \alpha}(t, \omega) d\omega \right) - f_k(t) \right| \leq D_W^{[1]} \tilde{\varepsilon}. \quad (12)$$

Remark 2. This theorem gives a strong approximation result for the class $\mathcal{A}_{\Delta, \varepsilon}$, tells us that the synchrosqueezing operator $S_{W_f^\psi}^{\lambda, \tilde{\varepsilon}, \alpha}$ is concentrated in narrow bands around the curves $(t, \frac{1}{\phi'_k(t)})$ in the TS plane and that the modes f_k s can be reconstructed from $S_{W_f^\psi}^{\lambda, \tilde{\varepsilon}, \alpha}$ with a reasonably high accuracy.

The proof of this theorem, for a compactly supported wavelet in the Fourier domain, was already proposed in [1] (with the slight difference that parameter α was not considered). For non compactly supported wavelet in the Fourier domain, the proof is similar in principle to that proposed for the short-time Fourier transform based synchrosqueezing (FSST) in [22], except of small changes that we will point out. The main ideas are briefly detailed hereafter.

First, we introduce the following proposition that is useful to prove item (a) of Theorem 1.

Proposition 1. For any $k \in \{1, \dots, K\}$ and $(t, a) \notin Z_k$, one has:

$$|W_{f_k}^\psi(t, a)| \leq \varepsilon E_{W,k}^{[1]}(t, a), \quad (13)$$

where $E_{W,k}^{[1]}(t, a) = aMJ_{1,0} + (\pi a^2 MJ_{2,0} + N_0)A_k(t)$ and $J_{n,p} = \int_{\mathbb{R}} |u|^n |\psi^{(p)}(u)| du$. Consequently, for any $(t, a) \in Z_k$:

$$|W_f^\psi(t, a) - W_{f_k}^\psi(t, a)| \leq \varepsilon \sum_{l \neq k} E_{W,l}^{[1]}(t, a) := \varepsilon \Omega_{W,k}^{[1]}(t, a). \quad (14)$$

Furthermore, for any $k \in \{1, \dots, K\}$ and $(t, a) \in \mathbb{R} \times \mathbb{R}_+$, one has:

$$|W_{f_k}^\psi(t, a) - W_{f_{k,1}}^\psi(t, a)| \leq \varepsilon \Gamma_{W,k,0}^{[1]}(t, a), \quad (15)$$

where $W_{f_{k,1}}^\psi(t, a) = f_k(t) \hat{\psi}(a\phi'_k(t))^*$ and $\Gamma_{W,k,0}^{[1]}(t, a) = aMJ_{1,0} + \pi a^2 MJ_{2,0} A_k(t)$.

Proof. For each $k \in \{1, \dots, K\}$, a zeroth order Taylor expansion of the amplitude and first order expansion of the phase of f_k leads to:

$$\begin{aligned} f_k(\tau) &= A_k(\tau) e^{i2\pi\phi_k(\tau)} \\ &= A_k(t) e^{i2\pi[\phi_k(t) + \phi'_k(t)(\tau-t)]} + (A_k(\tau) - A_k(t)) e^{i2\pi\phi_k(\tau)} \\ &\quad + A_k(t) [e^{i2\pi[\phi_k(t) + \phi'_k(t)(\tau-t) + \int_t^\tau \phi''_k(x)(\tau-x)dx]} - e^{i2\pi[\phi_k(t) + \phi'_k(t)(\tau-t)]}] \\ &= f_{k,1}(\tau) + f_{k,2}(\tau) + f_{k,3}(\tau). \end{aligned}$$

Then, for any (t, a) , the first term can be written as:

$$W_{f_{k,1}}^\psi(t, a) = \frac{1}{a} A_k(t) e^{i2\pi\phi_k(t)} \int_{\mathbb{R}} e^{i2\pi\phi'_k(t)(\tau-t)} \psi\left(\frac{\tau-t}{a}\right)^* d\tau = f_k(t) \hat{\psi}(a\phi'_k(t))^*.$$

The second term is bounded by:

$$\begin{aligned} |W_{f_{k,2}}^\psi(t, a)| &\leq \frac{1}{a} \int_{\mathbb{R}} |A_k(\tau) - A_k(t)| \left| \psi\left(\frac{\tau-t}{a}\right) \right| d\tau \\ &\leq \frac{\varepsilon M}{a} \int_{\mathbb{R}} |\tau-t| \left| \psi\left(\frac{\tau-t}{a}\right) \right| d\tau = \varepsilon a M J_{1,0}. \end{aligned}$$

and the third term by:

$$\begin{aligned} |W_{f_{k,3}}^\psi(t, a)| &\leq \frac{2\pi A_k(t)}{a} \int_{\mathbb{R}} \left(\int_t^\tau |\phi''_k(u)| |(\tau-u)| du \right) \left| \psi\left(\frac{\tau-t}{a}\right) \right| d\tau \\ &\leq \frac{\varepsilon \pi M A_k(t)}{a} \int_{\mathbb{R}} |\tau-t|^2 \left| \psi\left(\frac{\tau-t}{a}\right) \right| d\tau = \varepsilon \pi a^2 M J_{2,0} A_k(t). \end{aligned}$$

For $(t, a) \notin Z_k$, the assumptions on ψ lead to $|W_{f,k,1}^\psi(t, a)| \leq \varepsilon N_0 A_k(t)$. Additionally, using the linearity of CWT, one gets (13), and inequality (14) follows. Furthermore, if $(t, a) \in \mathbb{R} \times \mathbb{R}_+$, inequality (15) is also straightforward. \square

Remark 3. Note that $E_{W,k}^{[1]}(t, a)$, $\Omega_{W,k}^{[1]}(t, a)$, and $\Gamma_{W,k,0}^{[1]}(t, a)$ are uniformly bounded for $(t, a) \in \mathbb{E}$ because a is lower than α . In the seminal paper of Daubechies [1], this constraint on a was missing.

Now we can prove item (a) of Theorem 1: Since $E_{W,l}^{[1]}(t, a)$ is bounded on \mathbb{E} , we can consider:

$$\tilde{\varepsilon} \leq \left\| \sum_{l=1}^K E_{W,l}^{[1]}(t, a) \right\|_{\infty, \mathbb{E} \setminus \bigcup_{l=1}^K Z_l}^{-\frac{1}{2}}, \quad (16)$$

where $\|z(t, a)\|_{\infty, X} = \sup_{(t,a) \in X} |z(t, a)|$. For $(t, a) \in \mathbb{E} \setminus \bigcup_{l=1}^K Z_l$, we immediately get:

$$|W_f^\psi(t, a)| \leq \varepsilon \sum_{l=1}^K E_{W,l}^{[1]}(t, a) \leq \tilde{\varepsilon}.$$

Thus, if $|W_f^\psi(t, a)| > \tilde{\varepsilon}$, there is at least one k such that $(t, a) \in Z_k$. Furthermore, because of the separation condition on the modes, one can easily show the Z_k s are disjoint sets, so k is unique.

Let us now consider the following proposition that is useful to prove item (b) of Theorem 1.

Proposition 2. For $(t, a) \in Z_k$, assuming ψ satisfies the hypotheses of Theorem 2, one has:

$$\left| W_f^{\psi'}(t, a) + i2\pi a \phi'_k(t) W_f^\psi(t, a) \right| \leq \varepsilon B_{W,k}^{[1]}(t, a), \quad (17)$$

where

$$\begin{aligned} B_{W,k}^{[1]}(t, a) &= aMKJ_{0,0} + 2\pi a^2 M J_{1,0} \sum_{k=1}^K \|A_k\|_\infty \\ &\quad + 2\pi a \sum_{l \neq k} \phi'_l(t) E_{W,l}^{[1]}(t, a) + 2\pi a \phi'_k(t) \Omega_{W,k}^{[1]}(t, a). \end{aligned}$$

Proof. Differentiating the CWT of f with respect to t , we get for any (t, a) :

$$\begin{aligned}
\partial_t W_f^\psi(t, a) &= \frac{1}{a} \sum_{k=1}^K \int_{\mathbb{R}} A'_k(\tau) e^{i2\pi\phi_k(\tau)} \psi\left(\frac{\tau-t}{a}\right)^* d\tau \\
&\quad + \frac{1}{a} \sum_{k=1}^K \int_{\mathbb{R}} A_k(\tau) i2\pi\phi'_k(\tau) e^{i2\pi\phi_k(\tau)} \psi\left(\frac{\tau-t}{a}\right)^* d\tau \\
&= \frac{1}{a} \sum_{k=1}^K \int_{\mathbb{R}} A'_k(\tau) e^{i2\pi\phi_k(\tau)} \psi\left(\frac{\tau-t}{a}\right)^* d\tau \\
&\quad + \frac{1}{a} \sum_{k=1}^K \int_{\mathbb{R}} A_k(\tau) i2\pi \left[\phi'_k(t) + \int_t^\tau \phi''_k(u) du \right] e^{i2\pi\phi_k(\tau)} \psi\left(\frac{\tau-t}{a}\right)^* d\tau \\
&= \frac{1}{a} \sum_{k=1}^K \int_{\mathbb{R}} A'_k(\tau) e^{i2\pi\phi_k(\tau)} \psi\left(\frac{\tau-t}{a}\right)^* d\tau + i2\pi \sum_{k=1}^K \phi'_k(t) W_{f_k}^\psi(t, a) \\
&\quad + \frac{1}{a} \sum_{k=1}^K \int_{\mathbb{R}} A_k(\tau) i2\pi \left(\int_t^\tau \phi''_k(u) du \right) e^{i2\pi\phi_k(\tau)} \psi\left(\frac{\tau-t}{a}\right)^* d\tau.
\end{aligned}$$

Note that since $\partial_t W_f^\psi(t, a) = -\frac{1}{a} W_f^{\psi'}(t, a)$, one may then write:

$$\begin{aligned}
&\left| W_f^{\psi'}(t, a) + i2\pi a \sum_{k=1}^K \phi'_k(t) W_{f_k}^\psi(t, a) \right| \\
&\leq \sum_{k=1}^K \int_{\mathbb{R}} |A'_k(\tau)| \left| \psi\left(\frac{\tau-t}{a}\right) \right| d\tau + 2\pi \sum_{k=1}^K \int_{\mathbb{R}} A_k(\tau) \left(\int_t^\tau |\phi''_k(u)| du \right) \left| \psi\left(\frac{\tau-t}{a}\right) \right| d\tau \\
&\leq \varepsilon \left(aMKJ_{0,0} + 2\pi a^2 MJ_{1,0} \sum_{k=1}^K \|A_k\|_\infty \right).
\end{aligned}$$

From Proposition 1, we first have, when $(t, a) \in Z_k$:

$$\begin{aligned}
&\left| W_f^{\psi'}(t, a) + i2\pi a \phi'_k(t) W_{f_k}^\psi(t, a) \right| \\
&\leq \varepsilon \left(aMKJ_{0,0} + 2\pi a^2 MJ_{1,0} \sum_{k=1}^K \|A_k\|_\infty + 2\pi a \sum_{l \neq k} \phi'_l(t) E_{W,l}^{[1]}(t, a) \right),
\end{aligned}$$

and then,

$$\begin{aligned}
& \left| W_f^{\psi'}(t, a) + i2\pi a \phi'_k(t) W_f^\psi(t, a) \right| \\
& \leq \varepsilon \left(aMKJ_{0,0} + 2\pi a^2 MJ_{1,0} \sum_{k=1}^K \|A_k\|_\infty \right. \\
& \quad \left. + 2\pi a \sum_{l \neq k} \phi'_l(t) E_{W,l}^{[1]}(t, a) + 2\pi a \phi'_k(t) \Omega_{W,k}^{[1]}(t, a) \right),
\end{aligned}$$

which results in (17). \square

Now, we can prove item (b) of Theorem 1.

One can write for (t, a) satisfying $|W_f^\psi(t, a)| > \tilde{\varepsilon}$:

$$\begin{aligned}
\left| \hat{\omega}_{W_f^\psi}(t, a) - \phi'_k(t) \right| &= \left| -\frac{1}{i2\pi a} \frac{W_f^{\psi'}(t, a)}{W_f^\psi(t, a)} - \phi'_k(t) \right| \\
&= \left| \frac{1}{i2\pi a} \frac{W_f^{\psi'}(t, a) + i2\pi a \phi'_k(t) W_f^\psi(t, a)}{W_f^\psi(t, a)} \right| \\
&\leq \varepsilon \frac{B_{W,k}^{[1]}(t, a)}{|2\pi a W_f^\psi(t, a)|} \leq \tilde{\varepsilon}^2 \frac{B_{W,k}^{[1]}(t, a)}{2\pi a}.
\end{aligned}$$

By choosing

$$\tilde{\varepsilon} \leq \left\| \frac{B_{W,k}^{[1]}(t, a)}{2\pi a} \right\|_{\infty, \bigcup_{l=1}^K Z_l}^{-1}, \tag{18}$$

because $\frac{B_{W,k}^{[1]}(t, a)}{a}$ is bounded on $\bigcup_{l=1}^K Z_l$. For $(t, a) \in Z_k$ such that $|W_f^\psi(t, a)| > \tilde{\varepsilon}$, we immediately get:

$$\left| \hat{\omega}_{W_f^\psi}(t, a) - \phi'_k(t) \right| \leq \tilde{\varepsilon}. \tag{19}$$

Let us now consider the following lemma, which is useful to prove item (c) of Theorem 1.

Lemma 1. *Suppose that both (16) and (18) are satisfied, and that the following condition is also verified:*

$$\varepsilon \leq 1/8\Delta^3(\phi'_1(t) + \phi'_2(t))^3. \quad (20)$$

Consider the following sets:

$$\begin{aligned} \mathbb{X} &= \{a \in [0, \alpha] \text{ s.t. } |W_f^\psi(t, a)| > \tilde{\varepsilon} \text{ and } |\hat{\omega}_{W_f^\psi}(t, a) - \phi'_k(t)| \leq \tilde{\varepsilon}\}, \\ \mathbb{Y} &= \{a \text{ s.t. } |W_f^\psi(t, a)| > \tilde{\varepsilon} \text{ and } |a\phi'_k(t) - 1| < \Delta\}, \end{aligned}$$

then $\mathbb{X} = \mathbb{Y}$.

Proof. If $a \in \mathbb{X}$, it is such that $|W_f^\psi(t, a)| > \tilde{\varepsilon}$ and since $(t, a) \in \mathbb{E}$, from (a), (t, a) belongs to one Z_k . If $l \neq k$, one would have:

$$\begin{aligned} |\hat{\omega}_{W_f^\psi}(t, a) - \phi'_k(t)| &\geq |\phi'_l(t) - \phi'_k(t)| - |\hat{\omega}_{W_f^\psi}(t, a) - \phi'_l(t)| \\ &\geq \Delta(\phi'_l(t) + \phi'_k(t)) - \tilde{\varepsilon}. \end{aligned}$$

Condition (20) implies that, for all $k, l \in \{1, \dots, K\}$: $\Delta(\phi'_k(t) + \phi'_l(t)) > 2\tilde{\varepsilon}$. Thus, it leads to $|\hat{\omega}_{W_f^\psi}(t, a) - \phi'_k(t)| > \tilde{\varepsilon}$, which contradicts $a \in \mathbb{X}$. Hence, $l = k$ and $\mathbb{X} \subset \mathbb{Y}$. Conversely, if $a \in \mathbb{Y}$, equation (19) immediately shows $a \in \mathbb{X}$, hence $\mathbb{X} = \mathbb{Y}$. \square

Coming back to the proof of item (c) of Theorem 1, we let $t \in \mathbb{R}$ and note that $W_f^\psi(t, a) \in L^\infty(\mathbb{X})$. Then, since $a > 0$ on \mathbb{X} , $\frac{1}{a}W_f^\psi(t, a) \in L^1(\mathbb{X})$, and, thus, using the same type of technique as in [1] (Estimate 3.9), one can write:

$$\lim_{\lambda \rightarrow 0} \left(\int_{|\omega - \phi'_k(t)| < \tilde{\varepsilon}} S_{W_f^\psi}^{\lambda, \tilde{\varepsilon}, \alpha}(t, \omega) d\omega \right) = \frac{1}{C'_\psi} \int_{\mathbb{X}} W_f^\psi(t, a) \frac{da}{a}.$$

From this, we deduce:

$$\begin{aligned}
& \left| \lim_{\lambda \rightarrow 0} \left(\int_{|\omega - \phi'_k(t)| < \tilde{\varepsilon}} S_{W_f^\psi}^{\lambda, \tilde{\varepsilon}, \alpha}(t, \omega) d\omega \right) - f_k(t) \right| \\
& \leq \left| \frac{1}{C'_\psi} \int_{\{a \text{ s.t. } |a\phi'_k(t)-1| < \Delta\}} W_f^\psi(t, a) \frac{da}{a} - f_k(t) \right| \\
& \quad + \left| \frac{1}{C'_\psi} \int_{\{a \text{ s.t. } |W_f^\psi(t, a)| \leq \tilde{\varepsilon} \text{ and } |a\phi'_k(t)-1| < \Delta\}} W_f^\psi(t, a) \frac{da}{a} \right| \\
& \leq \frac{1}{|C'_\psi|} \int_{\{a \text{ s.t. } |a\phi'_k(t)-1| < \Delta\}} |W_f^\psi(t, a) - W_{f_k}^\psi(t, a)| \frac{da}{a} \\
& \quad + \frac{1}{|C'_\psi|} \int_{\{a \text{ s.t. } |a\phi'_k(t)-1| < \Delta\}} |W_{f_k}^\psi(t, a) - W_{f_{k,1}}^\psi(t, a)| \frac{da}{a} \\
& \quad + \left| \frac{1}{C'_\psi} \int_{\{a \text{ s.t. } |a\phi'_k(t)-1| < \Delta\}} f_k(t) \hat{\psi}(a\phi'_k(t))^* \frac{da}{a} - f_k(t) \right| + \frac{\tilde{\varepsilon}}{|C'_\psi|} \log \left(\frac{1+\Delta}{1-\Delta} \right) \\
& \leq \frac{1}{|C'_\psi|} \left[\int_{\{a \text{ s.t. } |a\phi'_k(t)-1| < \Delta\}} \Omega_{W,k}^{[1]}(t, a) \frac{da}{a} + \int_{\{a \text{ s.t. } |a\phi'_k(t)-1| < \Delta\}} \Gamma_{W,k,0}^{[1]}(t, a) \frac{da}{a} \right. \\
& \quad \left. + A_k(t) \left| \int_{\eta \text{ s.t. } |\eta-1| > \Delta} |\hat{\psi}(\tau)(\eta)^*| \frac{d\eta}{\eta} \right| + \tilde{\varepsilon} \log \left(\frac{1+\Delta}{1-\Delta} \right) \right] \\
& \leq \frac{1}{|C'_\psi|} \left[\left(\left\| \Omega_{W,k}^{[1]}(t, a) \right\|_{\infty, \bigcup_{l=1}^K Z_l} + \left\| \Gamma_{W,k,0}^{[1]}(t, a) \right\|_{\infty, \bigcup_{l=1}^K Z_l} + 1 \right) \log \left(\frac{1+\Delta}{1-\Delta} \right) \right. \\
& \quad \left. + \max_k \|A_k\|_\infty N_1 \right] \tilde{\varepsilon} = D_W^{[1]} \tilde{\varepsilon}.
\end{aligned}$$

4. Second order wavelet-based SST (WSST2)

4.1. Second order IF estimate

Although WSST proves to be an efficient solution to enhance TF representations, its applicability is restricted to a class of MCS composed of slightly perturbed purely harmonic modes. To overcome this limitation, a recent extension of WSST was introduced based on a more accurate IF estimate, which is then used to define an improved synchrosqueezing operator, called *second-order wavelet-based synchrosqueezing transform* (WSST2) [2].

More precisely, a second-order local modulation operator is first defined and then used to compute the new IF estimate. This modulation operator corresponds to the ratio of the first-order derivatives, with respect to t , of the reassignment operators, as explained in the following:

Proposition 3. *Given a signal $f \in L^\infty(\mathbb{R})$, the complex reassignment operators $\tilde{\omega}_{W_f^\psi}(t, a)$ and $\tilde{\tau}_{W_f^\psi}(t, a)$ are respectively defined for any (t, a) s.t. $W_f^\psi(t, a) \neq 0$ as:*

$$\tilde{\omega}_{W_f^\psi}(t, a) = \frac{1}{i2\pi} \frac{\partial_t W_f^\psi(t, a)}{W_f^\psi(t, a)} \quad (21)$$

$$\tilde{\tau}_{W_f^\psi}(t, a) = \frac{\int_{\mathbb{R}} \tau f(\tau) \frac{1}{a} \psi\left(\frac{\tau-t}{a}\right)^* d\tau}{W_f^\psi(t, a)} = t + a \frac{W_f^{t\psi}(t, a)}{W_f^\psi(t, a)}, \quad (22)$$

which are defined provided $t\psi$ and ψ' are in $L^1(\mathbb{R})$. Then, the second-order local complex modulation operator $\tilde{q}_{t, W_f^\psi}(t, a)$ is defined by:

$$\tilde{q}_{t, W_f^\psi}(t, a) = \frac{\partial_t \tilde{\omega}_{W_f^\psi}(t, a)}{\partial_t \tilde{\tau}_{W_f^\psi}(t, a)}, \quad \text{whenever } \partial_t \tilde{\tau}_{W_f^\psi}(t, a) \neq 0. \quad (23)$$

In that case, the definition of the improved IF estimate associated with the TF representation given by CWT is derived as:

Definition 3. *Let $f \in L^\infty(\mathbb{R})$, the second-order local complex IF estimate of f is defined as:*

$$\tilde{\omega}_{t, W_f^\psi}^{[2]}(t, a) = \begin{cases} \tilde{\omega}_{W_f^\psi}(t, a) + \tilde{q}_{t, W_f^\psi}(t, a)(t - \tilde{\tau}_{W_f^\psi}(t, a)) & \text{if } \partial_t \tilde{\tau}_{W_f^\psi}(t, a) \neq 0 \\ \tilde{\omega}_{W_f^\psi}(t, a) & \text{otherwise.} \end{cases} \quad (24)$$

Then, its real part $\hat{\omega}_{t, W_f^\psi}^{[2]}(t, a) = \Re\{\tilde{\omega}_{t, W_f^\psi}^{[2]}(t, a)\}$ is the desired IF estimate.

It was demonstrated in [2] that $\Re\left\{\tilde{q}_{t, W_f^\psi}(t, a)\right\} = \phi''(t)$ when f is a Gaussian modulated linear chirp, i.e. $f(t) = A(t)e^{i2\pi\phi(t)}$ where both $\log(A(t))$ and

$\phi(t)$ are quadratic. Also, $\Re\{\tilde{\omega}_{t,W_f^\psi}^{[2]}(t,a)\}$ is an exact estimate of $\phi'(t)$ for this kind of signals. For a more general mode with Gaussian amplitude, its IF can be estimated by $\Re\{\tilde{\omega}_{t,W_f^\psi}^{[2]}(t,a)\}$, in which the estimation error only involves the derivatives of the phase with orders larger than 3. Furthermore, $\tilde{\omega}_{W_f^\psi}(t,a)$ and $\tilde{q}_{t,W_f^\psi}(t,a)$ can be computed by means of only five CWTs as follows:

Proposition 4. *Let $f \in L^\infty(\mathbb{R})$, $\tilde{\omega}_{W_f^\psi}(t,a)$ and $\tilde{q}_{t,W_f^\psi}(t,a)$ can be written as:*

$$\tilde{\omega}_{W_f^\psi}(t,a) = -\frac{1}{i2\pi a} \frac{W_f^{\psi'}(t,a)}{W_f^\psi(t,a)} \quad (25)$$

$$\tilde{q}_{t,W_f^\psi}(t,a) = \frac{1}{i2\pi a^2} \frac{W_f^{\psi''}(t,a)W_f^\psi(t,a) - W_f^{\psi'}(t,a)^2}{W_f^{t\psi}(t,a)W_f^{\psi'}(t,a) - W_f^{t\psi'}(t,a)W_f^\psi(t,a)}, \quad (26)$$

where $t \mapsto W^{\psi'}, W^{t\psi}, W^{\psi''}, W^{t\psi'}$ are respectively CWTs of f computed with windows $\psi', t\psi, \psi'', t\psi'$ all in $L^1(\mathbb{R})$.

Proof. These expressions are easily derived using $\partial_t^p W_f^\psi(t,a) = \left(-\frac{1}{a}\right)^p W_f^{\psi^{(p)}}(t,a)$. \square

The second-order WSST (WSST2) is then defined by simply replacing $\hat{\omega}_{W_f^\psi}(t,a)$ by $\hat{\omega}_{t,W_f^\psi}^{[2]}(t,a)$ in (7):

$$S_{2,W_f^\psi}^{\gamma,\alpha}(t,\omega) := \frac{1}{C_\psi'} \int_{\mathbb{A}(\gamma,\alpha)} W_f^\psi(t,a) \delta\left(\omega - \hat{\omega}_{t,W_f^\psi}^{[2]}(t,a)\right) \frac{da}{a}, \quad (27)$$

and f_k is finally retrieved by replacing $S_{W_f^\psi}^{\gamma,\alpha}(t,\omega)$ by $S_{2,W_f^\psi}^{\gamma,\alpha}(t,\omega)$ in (8).

4.2. Mathematical foundations for WSST2

This section begins with the definition of another class of chirp-like functions, larger than $\mathcal{A}_{\Delta,\varepsilon}$ and that can be successfully dealt with WSST2:

Definition 4. *Let $\varepsilon > 0$ and $\Delta \in (0,1)$. The set $\mathcal{A}_{\Delta,\varepsilon}^{[2]}$ of multicomponent signals with second order modulation ε and separation Δ corresponds to the signals defined in (4) satisfying:*

(a) f_k is such that A_k and ϕ_k satisfy the following conditions:

$$\begin{aligned} A_k(t) &\in C^2(\mathbb{R}) \cap L^\infty(\mathbb{R}), \quad \phi_k(t) \in C^3(\mathbb{R}), \\ \phi'_k(t), \phi''_k(t), \phi'''_k(t) &\in L^\infty(\mathbb{R}), \\ A_k(t) &> 0, \quad \inf_{t \in \mathbb{R}} \phi'_k(t) > 0, \quad \sup_{t \in \mathbb{R}} \phi'_k(t) < \infty, \quad M = \max_k \left(\sup_{t \in \mathbb{R}} \phi'_k(t) \right), \\ |A'_k(t)| &\leq \varepsilon \phi'_k(t) \leq \varepsilon M, \quad |A''_k(t)| \leq \varepsilon \phi'_k(t) \leq \varepsilon M, \\ \text{and } |\phi'''_k(t)| &\leq \varepsilon \phi'_k(t) \leq \varepsilon M \quad \forall t \in \mathbb{R}. \end{aligned}$$

(b) the ϕ_k s satisfy the following separation condition

$$\phi'_{k+1}(t) - \phi'_k(t) \geq \Delta(\phi'_{k+1}(t) + \phi'_k(t)), \forall t \in \mathbb{R}, \quad \forall k \in \{1, \dots, K-1\}.$$

Now, let us define the second order WSST as follows:

Definition 5. Let h be a positive L^1 -normalized window belonging to $C_c^\infty(\mathbb{R})$, and consider $\gamma, \lambda > 0$, the second order WSST of f with threshold γ and accuracy λ is defined by:

$$S_{2, W_f^\psi}^{\lambda, \gamma, \alpha}(t, \omega) := \frac{1}{C_\psi'} \int_{\mathbb{A}(\gamma, \alpha)} W_f^\psi(t, a) \frac{1}{\lambda} h \left(\frac{\omega - \hat{\omega}_{t, W_f^\psi}^{[2]}(t, a)}{\lambda} \right) \frac{da}{a}. \quad (28)$$

In Section 3, we showed that, for functions $f \in \mathcal{A}_{\Delta, \varepsilon}$, a good IF estimate was given by $\hat{\omega}_{W_f^\psi}(t, a)$ and the approximation theorem followed. Here, to assess the approximation property of the second order WSST we have just introduced, we consider $f \in \mathcal{A}_{\Delta, \varepsilon}^{[2]}$ for which we are going to prove that $\hat{\omega}_{W_f^\psi}^{[2]}(t, a)$ is a good IF estimate. The approximation theorem is as follows:

Theorem 2. Consider $f \in \mathcal{A}_{\Delta, \varepsilon}^{[2]}$, set $\tilde{\varepsilon} = \varepsilon^{1/6}$. Let ψ be a wavelet satisfying, for $r \in \{0, 1\}$ and $p \in \{0, 1\}$, $|\mathcal{F}\{\tau^r \psi^{(p)}(\tau) e^{-i\pi \phi_k''(t) a^2 \tau^2}\}(\eta)| \leq K_{W, r, p} \varepsilon$ when $|\eta - 1| > \Delta$, and $\int_{\{\eta \text{ s.t. } |\eta - 1| > \Delta\}} |\mathcal{F}\{\psi(\tau) e^{-i\pi \phi_k''(t) a^2 \tau^2}\}(\eta)^*| \frac{d\eta}{\eta} \leq K_{W, 3} \tilde{\varepsilon}$, for some constants $K_{W, r, p}$ and $K_{W, 3}$ and where \mathcal{F} denotes the Fourier transform.

Assuming $(t, a) \in \mathbb{E}$, then, provided ε is sufficiently small, the following hold:

- (a) $|W_f^\psi(t, a)| > \tilde{\varepsilon}$ on \mathbb{E} only when, there exists $k \in \{1, \dots, K\}$, such that $(t, a) \in Z_k := \{(t, a), \text{ s.t. } |a\phi'_k(t) - 1| < \Delta\}$.
- (b) For each $k \in \{1, \dots, K\}$ and for all $(t, a) \in Z_k$, for which hold $|W_f^\psi(t, a)| > \tilde{\varepsilon}$ and $|\partial_t \tilde{\tau}_{W_f^\psi}(t, a)| > \tilde{\varepsilon}$, one has

$$|\hat{\omega}_{t, W_f^\psi}^{[2]}(t, a) - \phi'_k(t)| \leq \tilde{\varepsilon}. \quad (29)$$

- (c) Moreover, for each $k \in \{1, \dots, K\}$, there exists a constant $D_W^{[2]}$ such that

$$\left| \left(\lim_{\lambda \rightarrow 0} \int_{|\omega - \phi'_k(t)| < \tilde{\varepsilon}} S_{2, W_f^\psi}^{\lambda, \tilde{\varepsilon}, \alpha}(t, \omega) d\omega \right) - f_k(t) \right| \leq D_W^{[2]} \tilde{\varepsilon}. \quad (30)$$

Remark 4. It is worth noting that the same study carried out on in the STFT context required hypotheses on the window used that did not involve the frequency [22] [see Theorem 4] contrary to the wavelet case where the hypotheses involve the scale a .

The proof of Theorem 2 is available in Section Appendix .

5. Variants of second-order SST

5.1. Wavelet-based modulation operator using differentiation with respect to scale

By using partial derivatives with respect to a instead of t , a new second-order local modulation operator $\tilde{q}_{a, W_f^\psi}(t, a)$ showing the same properties as those of $\tilde{q}_{t, W_f^\psi}(t, a)$ can be obtained as follows:

Definition 6. Given a signal $f \in L^\infty(\mathbb{R})$, the second-order local complex modulation operator \tilde{q}_{a, W_f^ψ} is defined by:

$$\tilde{q}_{a, W_f^\psi}(t, a) = \frac{\partial_a \tilde{\omega}_{W_f^\psi}(t, a)}{\partial_a \tilde{\tau}_{W_f^\psi}(t, a)} \quad \text{whenever } \partial_a \tilde{\tau}_{W_f^\psi}(t, a) \neq 0, \quad (31)$$

where $\tilde{\omega}_{W_f^\psi}(t, a)$ and $\tilde{\tau}_{W_f^\psi}(t, a)$ are respectively defined in (21).

Proposition 5. Let $f \in L^\infty(\mathbb{R})$, $\tilde{q}_{a,W_f^\psi}(t, a)$ can be written as:

$$\tilde{q}_{a,W_f^\psi}(t, a) = \frac{1}{i2\pi a^2} \frac{W_f^{(t\psi')'}(t, a)W_f^\psi(t, a) - W_f^{\psi'}(t, a)W_f^{t\psi'}(t, a)}{W_f^{t\psi}(t, a)W_f^{t\psi'}(t, a) - W_f^{t^2\psi'}(t, a)W_f^\psi(t, a)} \quad (32)$$

Proof. The expression is derived using $\partial_a W_f^\psi(t, a) = -\frac{1}{a}W_f^\psi(t, a) - \frac{1}{a}W_f^{t\psi'}(t, a)$, since we have:

$$\begin{aligned} \partial_a \tilde{\omega}_{W_f^\psi}(t, a) &= \frac{1}{i2\pi a^2} \frac{W_f^{(t\psi')'}(t, a)W_f^\psi(t, a) - W_f^{\psi'}(t, a)W_f^{t\psi'}(t, a)}{W_f^\psi(t, a)^2} \\ \partial_a \tilde{\tau}_{W_f^\psi}(t, a) &= \frac{W_f^{t\psi}(t, a)W_f^{t\psi'}(t, a) - W_f^{t^2\psi'}(t, a)W_f^\psi(t, a)}{W_f^\psi(t, a)^2} \end{aligned}$$

□

Then, a new IF estimate having the same properties as $\tilde{\omega}_{t,W_f^\psi}^{[2]}(t, a)$ is introduced as:

Definition 7. Let $f \in L^\infty(\mathbb{R})$, the second-order local complex IF estimate of signal f is defined by:

$$\tilde{\omega}_{a,W_f^\psi}^{[2]}(t, a) = \begin{cases} \tilde{\omega}_{W_f^\psi}(t, a) + \tilde{q}_{a,W_f^\psi}(t, a)(t - \tilde{\tau}_{W_f^\psi}(t, a)) & \text{if } \partial_a \tilde{\tau}_{W_f^\psi}(t, a) \neq 0 \\ \tilde{\omega}_{W_f^\psi}(t, a) & \text{otherwise.} \end{cases}$$

Then, its real part $\hat{\omega}_{a,W_f^\psi}^{[2]}(t, a) = \Re\{\tilde{\omega}_{a,W_f^\psi}^{[2]}(t, a)\}$ is the desired IF estimate.

It can again be shown that $\Re\{\tilde{q}_{a,W_f^\psi}(t, a)\}$ is an exact estimate of the modulation for a Gaussian modulated linear chirp, while $\hat{\omega}_{a,W_f^\psi}^{[2]}(t, a)$ exactly estimates the instantaneous frequency in such a case. A variant of second-order WSST is then defined by simply replacing $\hat{\omega}_{W_f^\psi}(t, a)$ by $\hat{\omega}_{a,W_f^\psi}^{[2]}(t, a)$ in (7):

$$S_{2,a,W_f^\psi}^{\gamma,\alpha}(t, \omega) := \frac{1}{C'_\psi} \int_{\mathbb{A}(\gamma,\alpha)} W_f^\psi(t, a) \delta\left(\omega - \hat{\omega}_{a,W_f^\psi}^{[2]}(t, a)\right) \frac{da}{a}, \quad (33)$$

and f_k is finally retrieved by replacing $S_{W_f^\psi}^{\gamma,\alpha}(t, \omega)$ by $S_{2,a,W_f^\psi}^{\gamma,\alpha}(t, \omega)$ in (8).

Remark 5. The approximation theorem for this variant can be derived similarly to Theorem 2, except item (b) uses condition $|\partial_a \tilde{\tau}_{W_f^\psi}(t, a)| > \tilde{\varepsilon}$ instead of $|\partial_t \tilde{\tau}_{W_f^\psi}(t, a)| > \tilde{\varepsilon}$.

5.2. STFT-based modulation operators

Originally introduced as a post-processing method applied to the CWT, SST can alternatively be applied to STFT with some minor changes to obtain FSST [21, 24]. Like WSST, FSST suffers from a somewhat limiting applicability due to the hypotheses of weak frequency modulation for the modes making up the signal. To better take into account the frequency modulation, an extension of FSST was introduced, based on a more accurate IF estimate computed using a second-order local modulation operator [25, 26]. This new synchrosqueezing operator was then theoretically studied in [22]. For the sake of consistency, we briefly recall the definition of FSST2, based on the STFT, whose definition follows:

Definition 8. Given a signal $f \in L^\infty(\mathbb{R})$ and a window $g \in L^1(\mathbb{R})$, the (modified) STFT of f is defined by:

$$V_f^g(t, \eta) = \int_{\mathbb{R}} f(\tau) g(\tau - t) e^{-2i\pi\eta(\tau - t)} d\tau. \quad (34)$$

The complex reassignment operators $\tilde{\omega}_{V_f^g}(t, \eta)$ and $\tilde{\tau}_{V_f^g}(t, \eta)$ then respectively correspond, for any (t, η) such that $V_f^g(t, \eta) \neq 0$, to:

$$\begin{aligned} \tilde{\omega}_{V_f^g}(t, \eta) &= \frac{\partial_t V_f^g(t, \eta)}{2i\pi V_f^g(t, \eta)} = \eta - \frac{1}{i2\pi} \frac{V_f^{g'}(t, \eta)}{V_f^g(t, \eta)} \\ \tilde{\tau}_{V_f^g}(t, \eta) &= t - \frac{\partial_\eta V_f^g(t, \eta)}{2i\pi V_f^g(t, \eta)} = t + \frac{V_f^{tg}(t, \eta)}{V_f^g(t, \eta)}. \end{aligned} \quad (35)$$

and, the second-order local complex modulation operator $\tilde{q}_{t, V_f^g}(t, \eta)$ to:

$$\begin{aligned} \tilde{q}_{t, V_f^g}(t, \eta) &= \frac{\partial_t \tilde{\omega}_{V_f^g}(t, \eta)}{\partial_t \tilde{\tau}_{V_f^g}(t, \eta)} \quad \text{whenever } \partial_t \tilde{\tau}_{V_f^g}(t, \eta) \neq 0 \\ &= \frac{1}{i2\pi} \frac{V_f^{g''} V_f^g - (V_f^{g'})^2}{V_f^{tg} V_f^{g'} - V_f^{tg'} V_f^g}, \end{aligned} \quad (36)$$

where V_f^g denotes $V_f^g(t, \eta)$ and $V_f^{g'}, V_f^{tg}, V_f^{g''}, V_f^{tg'}$ are respectively STFTs of f computed with windows $t \mapsto g'(t), tg(t), g''(t)$ and $tg'(t)$ (which are all supposed to be in $L^1(\mathbb{R})$).

It was already demonstrated in [22] that $\Re\{\tilde{\omega}_{t,V_f^g}^{[2]}(t, \eta)\}$ is a perfect estimate of the frequency modulation for a Gaussian modulated linear chirp. In that case, the definition of the improved associated IF estimate was derived as:

$$\tilde{\omega}_{t,V_f^g}^{[2]}(t, \eta) = \begin{cases} \tilde{\omega}_{V_f^g}(t, \eta) + \tilde{q}_{t,V_f^g}(t, \eta)(t - \tilde{\tau}_{V_f^g}(t, \eta)) & \text{if } \partial_t \tilde{\tau}_{V_f^g}(t, \eta) \neq 0 \\ \tilde{\omega}_{V_f^g}(t, \eta) & \text{otherwise.} \end{cases}$$

Then, its real part $\hat{\omega}_{t,V_f^g}^{[2]}(t, \eta) = \Re\{\tilde{\omega}_{t,V_f^g}^{[2]}(t, \eta)\}$ is the desired IF estimate. FSST2 was then defined by:

$$T_{2,V_f^g}^\gamma(t, \omega) = \frac{1}{g^*(0)} \int_{\{\eta \text{ s.t. } |V_f^g(t, \eta)| > \gamma\}} V_f^g(t, \eta) \delta\left(\omega - \hat{\omega}_{t,V_f^g}^{[2]}(t, \eta)\right) d\eta, \quad (37)$$

and mode f_k was finally retrieved through:

$$f_k(t) \approx \int_{\{\omega, |\omega - \varphi_k(t)| < d\}} T_{2,V_f^g}^\gamma(t, \omega) d\omega. \quad (38)$$

In a recent paper [27], the authors of this paper proposed another modulation operator $\tilde{q}_{\eta,V_f^g}(t, \eta)$, showing the same properties as those of $\tilde{q}_{t,V_f^g}(t, \eta)$, and derived using the partial derivatives with respect to η instead of t .

Proposition 6. *The second-order modulation operator $\tilde{q}_{\eta,V_f^g}(t, \eta)$ is defined by:*

$$\begin{aligned} \tilde{q}_{\eta,V_f^g} &= \frac{\partial_\eta \tilde{\omega}_{V_f^g}(t, \eta)}{\partial_\eta \tilde{\tau}_{V_f^g}(t, \eta)} \quad \text{whenever } \partial_\eta \tilde{\tau}_{V_f^g}(t, \eta) \neq 0, \\ &= \frac{1}{i2\pi} \frac{V_f^g V_f^{(tg)'} - V_f^{g'} V_f^{tg}}{V_f^g V_f^{t^2g} - (V_f^{tg})^2} \\ &= \frac{1}{i2\pi} \frac{(V_f^g)^2 + V_f^{tg'} V_f^g - V_f^{g'} V_f^{tg}}{V_f^g V_f^{t^2g} - (V_f^{tg})^2}, \end{aligned} \quad (39)$$

where V_f^g denotes $V_f^g(t, \eta)$ and $V_f^{g'}, V_f^{tg}, V_f^{tg'}$ are respectively STFTs of f computed with windows $t \mapsto g'(t), tg(t), tg'(t)$ and $t^2g(t)$, all supposed to be in $L^1(\mathbb{R})$.

A new IF estimate having the same properties as $\tilde{\omega}_{t,V_f^g}^{[2]}(t, \eta)$ is introduced as follows:

Definition 9. Let $f \in L^\infty(\mathbb{R})$, the second-order local complex IF estimate of signal f is defined by:

$$\tilde{\omega}_{\eta,V_f^g}^{[2]}(t, \eta) = \begin{cases} \tilde{\omega}_{V_f^g}(t, \eta) + \tilde{q}_{\eta,V_f^g}(t, \eta)(t - \tilde{\tau}_{V_f^g}(t, \eta)) & \text{if } \partial_\eta \tilde{\tau}_{V_f^g}(t, \eta) \neq 0 \\ \tilde{\omega}_{V_f^g}(t, \eta) & \text{otherwise.} \end{cases} \quad (40)$$

Then, its real part $\hat{\omega}_{\eta,V_f^g}^{[2]}(t, \eta) = \Re\{\tilde{\omega}_{\eta,V_f^g}^{[2]}(t, \eta)\}$ is the desired IF estimate.

Remark 6. If $g(t) = e^{-\lambda t^2}$ for some $\lambda > 0$, then one can easily check that $\tilde{q}_{t,V_f^g} = \tilde{q}_{\eta,V_f^g}$, whatever f . It is also easy to show that $\hat{\omega}_{\eta,V_f^g}^{[2]}(t, \eta)$ is an exact instantaneous frequency estimate for Gaussian modulated linear chirp.

Remark 7. The approximation theorems for this new type of second order FSST based on STFT can be derived similarly to what was done for FSST2 (see [22]) except that the approximation of the chirp rate is now valid only when $\partial_\eta \tilde{\tau}_{V_f^g}(t, \eta)$ is not too small.

6. Numerical analysis of the behavior of WSST2 and comparisons

In this section, we provide numerical experiments to demonstrate the efficiency of our new second order wavelet-based synchrosqueezing transform (WSST2) compared with other existing synchrosqueezing transforms on simulated signals. More precisely, we carry out a comparison in terms of concentration and accuracy of the TF representations obtained. For that purpose, we start with considering a complex simulated MCS (f) composed of three components: a linear chirp (f_1), an hyperbolic chirp (f_2) and an exponential chirp (f_3) with Gaussian modulated amplitudes, whose instantaneous frequencies are respectively linear ($\phi''(t) \propto cst$), hyperbolic ($\phi''(t) \propto \phi'(t)^2$) and exponential ($\phi''(t) \propto \phi'(t)$). Note that f_1 behaves locally as a Gaussian modulated linear chirp, while both f_2 and f_3 contain strong nonlinear frequency modulations.

In our simulations, f is sampled over time interval $[0, 1]$ with a sampling rate $M = 1024$ Hz. An arbitrary threshold $\gamma = \gamma_0 = 0.001$ is set for noise-free

signals (the results between relatively insensitive to that threshold). Also, we use the complex Morlet wavelet (*resp.* Gaussian window) to compute the CWT (*resp.* STFT), which depends on a parameter $\sigma_W = 5$ (*resp.* $\sigma_F = 0.05$) as follows:

$$\hat{\psi}(\eta) = \sigma_W^{\frac{1}{2}} e^{-\pi\sigma_W^2(1-\eta)^2} \text{ and } \hat{g}(\eta) = \sigma_F^{\frac{1}{2}} e^{-\pi\sigma_F^2\eta^2}.$$

Note that when using Morlet wavelet (*resp.* Gaussian window), the chirp rate estimates \tilde{q}_{t,W_f^ψ} and \tilde{q}_{a,W_f^ψ} (*resp.* \tilde{q}_{t,V_f^g} and \tilde{q}_{a,V_f^g}) show the same behavior on f , therefore we only display experiments on \tilde{q}_{t,W_f^ψ} and \tilde{q}_{t,V_f^g} for the sake of simplicity. Further, the wavelet-based (*resp.* STFT-based) synchrosqueezing transforms are represented on a logarithmic (*resp.* linear) scale. The Matlab codes for synchrosqueezing transforms and the scripts leading to all figures of this paper can be found <https://github.com/phamduonghung/WSST2>.

In Figures 1 (a), (b) and (c), we display respectively the real part of the three components along with their amplitudes, and, in Figure 1 (d), the real part of the whole signal.

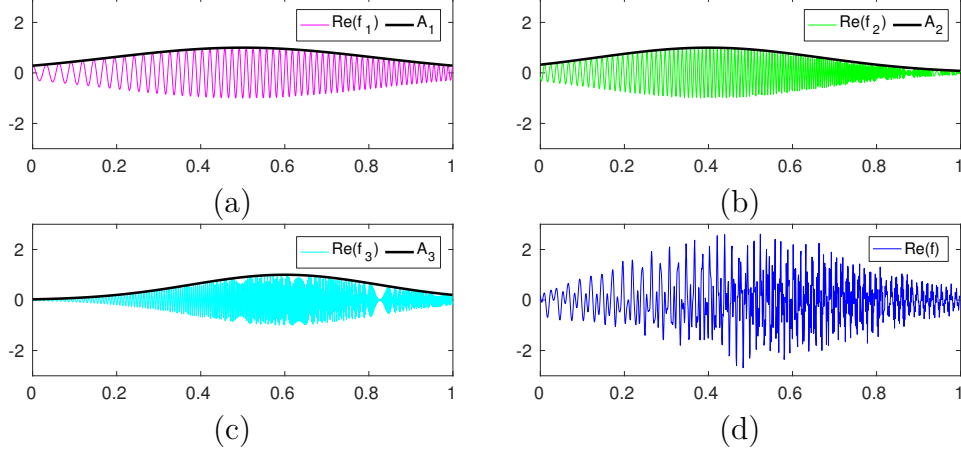


Figure 1: (a), (b) and (c): real part of f_1 , f_2 , and f_3 respectively with Gaussian modulated amplitudes A_1 , A_2 and A_3 superimposed; (d): real part of f .

We then display, still in the noise-free context, the CWT and STFT of f in the first column of Figure 2. Then, on the other two columns of this figure, the reassigned versions of the STFT and CWT given by some synchrosqueezing transforms mentioned in this paper are depicted.

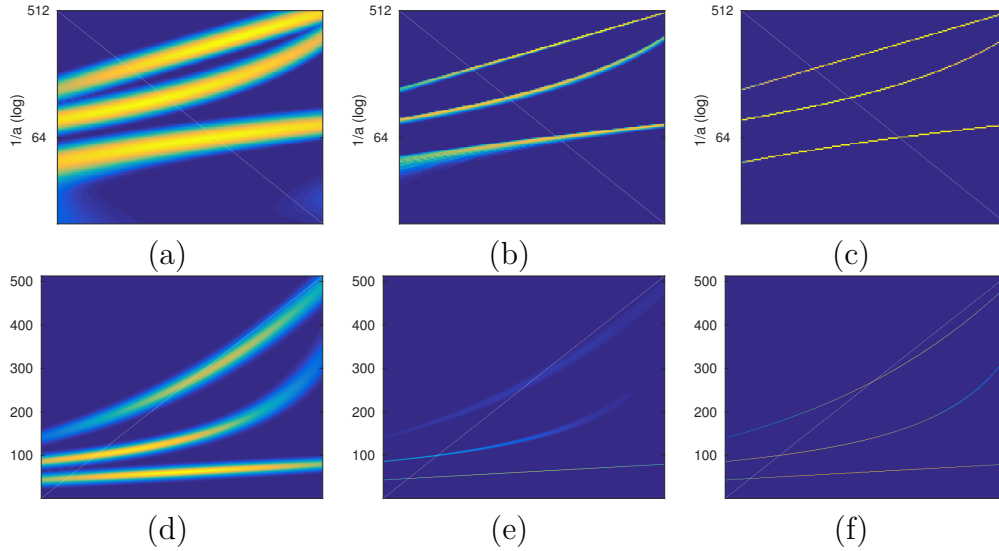


Figure 2: *First row*, (a): modulus of the CWT of f ; (b): WSST; (c) WSST2; *Second row*, (d): modulus of the STFT of f ; (e): FSST; (f): FSST2. Threshold $\gamma_0 = 0.001$.

Analyzing these figures, we first remark that, as expected, FSST leads to a relatively sharp TF representation for the linear chirp f_1 , that looks similar to the ones given by WSST2 and FSST2, and much better than that corresponding to WSST. However, FSST fails to reassign the STFT of f_2 and f_3 correctly where the IFs of these modes have non negligible frequency modulations. In contrast, the reassigned representations of f_2 and f_3 provided by WSST are much more concentrated at these locations. Moreover, it is of interest to remark that the quality of the representation corresponding to WSST seems not to depend on the scale for f_2 contrary to what happens with f_3 . Actually, this phenomenon is confirmed by the study available in [28], ch. 4, which says that to obtain a representation with constant quality, the mode must satisfy a constant ratio ϕ''/ϕ'^2 , which corresponds to a hyperbolic chirp. Finally, it can be seen that for f_2 and f_3 , both WSST2 and FSST2 seem to behave very similarly when considering either of the three studied modes, and result in compact TF representations.

For a better understanding of the performance improvement brought by the use of WSST2 over other studied methods, we introduce a quantitative comparison of all these techniques from the angle of energy concentration of TF representations carried out both on noise-free and noisy signals, and

then a measure of their localization accuracy by means of the Earth mover's distance (EMD).

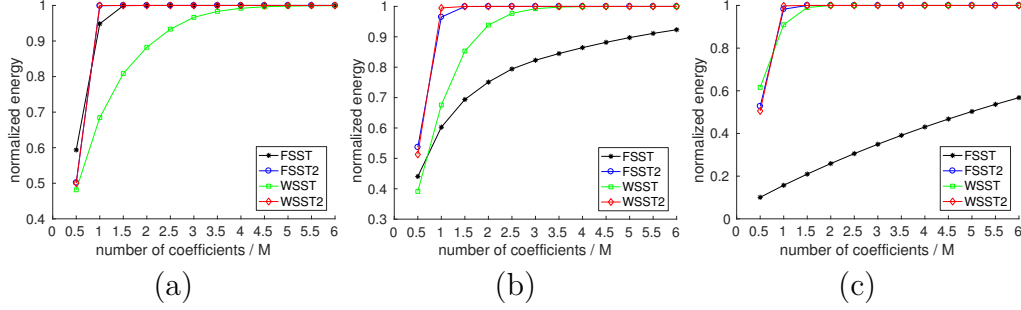


Figure 3: (a) Normalized energy as a function of the number of sorted TF coefficients for f_1 . Abscissa corresponds to the number of coefficients over the size M of the signal; (b): same as (a) but for f_2 ; (c): same as (a) but for f_3 . Threshold $\gamma_0 = 0.001$.

6.1. Evaluation of TF concentration

The TF concentration is one of the outstanding features used for evaluating the performance of the different TF techniques. To quantify this feature, an appealing method first introduced in [26] and then applied successfully in [27] is used in this paper. The main aim of such a method is to measure the energy concentration by considering the proportion of the latter contained in the first nonzero coefficients associated with the highest amplitudes, which we call *normalized energy*. When computed on a mono-component signal, the faster it increases towards 1 with the number of coefficients involved, the more concentrated the TF representation. In Figure 3 (a), we depict the normalized energy corresponding to the reassignment of the STFT of f_1 using different techniques, with respect to the number of coefficients kept divided by the length of f_1 (which corresponds to the sampling rate M in our case). From this figure, it can be checked again that, for f_1 , the energy is perfectly localized when using both WSST2 and FSST2, since they require only one coefficient per time instant to recover the signal energy, while WSST and FSST need more coefficients (5 and 2 respectively). The same computations carried out on f_2 and f_3 show that WSST2 still better performs than the other methods, especially WSST or FSST.

To further challenge the different TF reassigned techniques in the presence of noise, we consider a noisy signal $f_\zeta(t) = f(t) + \zeta(t)$, where $\zeta(t)$ is a complex

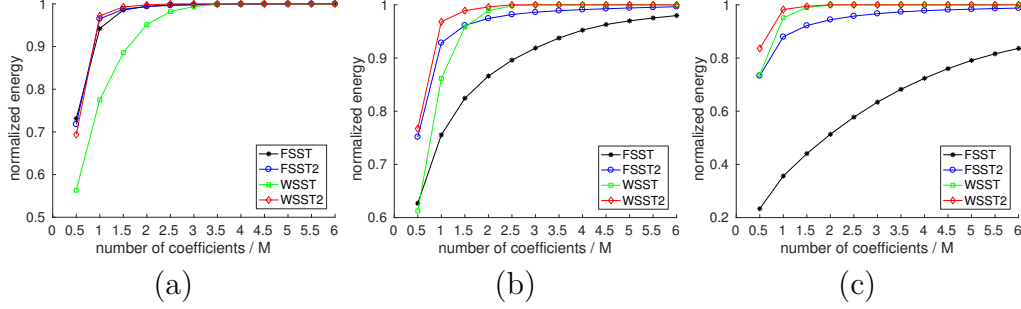


Figure 4: (a) Normalized energy as a function of the number of sorted TF coefficients for noisy f_1 (SNR= 0dB); (b): same as (a) but for noisy f_2 (at level 0dB); (c): same as (a) but for noisy f_3 (at level 0dB).

white Gaussian process with variance $\text{Var}(\Re\{\zeta(t)\}) = \text{Var}(\Im\{\zeta(t)\}) = \sigma_\zeta^2$, where $\Im\{Z\}$ is the imaginary part of complex number Z . Furthermore, the noise level is measured by the Signal-to-Noise Ratio (SNR):

$$\text{SNR}_{\text{input}}[\text{dB}] = 20 \log_{10} \frac{\|f\|_2}{\|f_\zeta - f\|_2}, \quad (41)$$

where $\|\cdot\|_2$ is the l_2 norm. Note also that in this noisy context, one of the well-known issue regarding the use of SST is the choice of an appropriate threshold γ on $W_f^\psi(t, a)$ or $V_f^g(t, \eta)$ in the definition of the synchrosqueezing operator to allow for signal denoising and a fair comparison between the different tested methods. Here, we propose a technique enabling adaptive determination of the threshold γ as a function of the noise level. Such a technique exploits the linearity of CWT and the fact that, for a fixed scale a , one has:

$$\text{std}(\Re\{W_\zeta^\psi(t, a)\}) = \sigma_\zeta \frac{1}{\sqrt{a}} \|\psi\|_2 \quad \text{and} \quad \text{std}(\Im\{W_\zeta^\psi(t, a)\}) = \sigma_\zeta \frac{1}{\sqrt{a}} \|\psi\|_2,$$

where std is the standard deviation. Thus, if one chooses a threshold $\gamma_W = 2\sigma_\zeta \frac{1}{\sqrt{a}} \|\psi\|_2$ for CWT, keeping only the coefficients satisfying:

$$\begin{aligned} |\Re\{W_{f_\zeta}^\psi(t, a)\}| > \gamma_W &= 2\sigma_\zeta \frac{1}{\sqrt{a}} \|\psi\|_2, \\ \text{and } |\Im\{W_{f_\zeta}^\psi(t, a)\}| > \gamma_W &= 2\sigma_\zeta \frac{1}{\sqrt{a}} \|\psi\|_2, \end{aligned}$$

in the synchrosqueezing transforms guarantees an efficient noise removal. The same arguments applied to STFT lead to keeping only the coefficients satisfying:

$$\left| \Re \left\{ V_{f_\zeta}^g(t, \eta) \right\} \right| > \gamma_F = 2\sigma_\zeta \|g\|_2,$$

and $\left| \Im \left\{ V_{f_\zeta}^g(t, \eta) \right\} \right| > \gamma_F = 2\sigma_\zeta \|g\|_2,$

in the definition of the synchrosqueezing transform.

Using the just defined threshold, we carry out the same numerical experiments regarding energy concentration as in the noise-free case, but each mode being contaminated by a white Gaussian noise (SNR = 0dB). The results displayed in Figure 4 exhibit a slightly slower growth of the normalized energy since the coefficients corresponding to noise, that the above technique cannot completely eliminate, are spread out over the whole TF or TS planes. However, the normalized energy is still more concentrated using WSST2 than the other methods, so that the former proves to be the most competitive of the tested reassignment techniques, even in the presence of heavy noise.

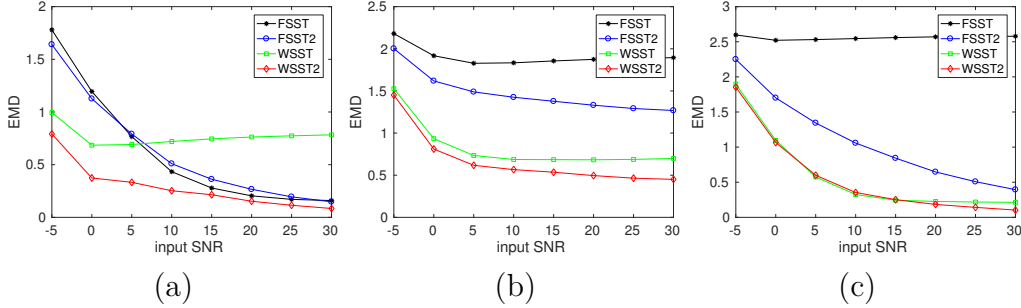


Figure 5: (a): EMD corresponding to different TF representations of f_1 either given by RM, FSST2, FSST3 or FSST4; (b): same as (a) but for f_2 ; (c): same as (a) but for f_3 .

Although quite informative, the normalized energy as illustrated in Figure 4 does not deliver any insight into the accuracy of the reassigned transforms. The latter can alternatively be quantified by measuring the dissimilarity between the resultant TF representations and the ideal one by means of the Earth mover's distance (EMD), a procedure already used in the synchrosqueezing context in [16]. The EMD is a sliced Wasserstein distance, commonly used in optimal transport, which allows for the comparison of two probability distributions. More precisely, it consists in computing the 1D EMD between the resultant TF representations and the ideal one, for each

individual time t , and then take the average over all t to define the global EMD. A smaller EMD means a better TF representation concentration to the ground truth and less noise fluctuations. In Figures 5 (a), (b) and (c), we display, respectively for the three modes already tested, the evolution of EMD with respect to the noise level, for TF representations given either by WSST, WSST2, FSST or FSST2. This study tells us that, for modes f_1 and f_2 , WSST2 always achieves the best performance whatever the input SNR. Moving to f_3 , WSST2 performs similarly to WSST at high noise level and is more accurate at low noise level, while it consistently outperforms FSST and FSST2. These results confirm the interest of using WSST2 on many different types of signals, even at high noise level noise.

6.2. Evaluation of mode reconstruction performance

Table 1: Accuracy of mode retrieval in the noise-free case

	FSST	FSST2	WSST	WSST2
Mode f_1	13.2	31.3	4.72	43.1
Mode f_2	1.68	17.4	6.03	23.6
Mode f_3	0.60	18.5	12.4	27.0
MCS f	3.09	19.8	6.48	27.1

Table 2: Accuracy of mode retrieval in the noisy case, (at noise level 0dB)

	FSST	FSST2	WSST	WSST2
Mode f_1	4.99	6.21	4.11	8.23
Mode f_2	2.42	6.51	5.71	8.67
Mode f_3	0.80	4.18	5.90	6.63
MCS f	2.55	5.41	5.08	7.83

As discussed above, the variants of second order SST proposed in this paper leading to significantly better TF representations, this should translate into better performance in terms of mode reconstruction. Let us first briefly

recall that f_k is retrieved from the TF representation of f given by the WSST2 (other SSTs have the same mode retrieval procedure) through:

$$f_k(t) \approx \int_{\{\omega, |\omega - \varphi_k(t)| < d\}} S_{2, W_f^\psi}^{\gamma, \alpha}(t, \omega) d\omega, \quad (42)$$

Note that $\varphi_k(t)$ is the estimate of $\phi'_k(t)$ given by the ridge detector (see [29] for details on such a technique used in this paper), and d is an integer parameter (because the frequency resolution is here associated with integer location) used to compensate for the inaccuracy of the estimate $\varphi_k(t)$ and also for the errors caused by approximating the IF by $\hat{\omega}_{t, W_f^\psi}^{[2]}(t, a)$. We first analyze the performance of the reconstruction procedure by considering the information on the ridge only, i.e. we take $d = 0$. For that purpose, we measure the output SNR, defined by $\text{SNR}_{\text{output}} = 20 \log_{10} \frac{\|f\|_2}{\|f_r - f\|_2}$, where f_r is the reconstructed signal. In Table 1, we display this output SNR for modes f_1, f_2, f_3 and also for f , using either FSST, FSST2, WSST or WSST2 for mode reconstruction. Further, we carry out the same experiments, but each mode is embedded in a white Gaussian noise at a noise level 0dB. The resultant accuracies for such a reconstruction are displayed in Table 2. From these results, we can see that the improvement brought by using WSST2 is clear and coherent with the previous study of the accuracy of the proposed new TF representations.

7. Conclusion

This paper introduced a novel synchrosqueezing transform for analyzing multicomponent signals made of strongly frequency-modulated modes, based on the continuous wavelet transform. It simply consists of a refinement of the instantaneous frequency estimate, computed using a second-order expansion of the phase. After having revisited the case of first-order synchrosqueezing, releasing the hypothesis of a wavelet compactly supported in the frequency domain, we proved a novel approximation theorem involving the proposed new synchrosqueezing transform applied to multicomponent signals made of strongly modulated modes. Numerical experiments showed the benefits of taking into account frequency modulation for both representation and reconstruction purposes. Future work should now be devoted to the theoretical analysis of the behavior of the proposed representations when applied to

noisy signals, as was done in [30, 31] for the original WSST. In this regard, it would also be of interest to study the behavior of the transform when the type of noise is non Gaussian.

Appendix

Theorem 2 is a generalization of Theorem 1, so the proof of the former is in principle similar to that of the latter. Proposition 1 generalizes into:

Proposition 7. *For any $k \in \{1, \dots, K\}$, any $r \in \{0, 1\}$ and $p \in \{0, 1\}$, and $(t, a) \notin Z_k$, one has:*

$$\left| W_{f_k}^{t^r \psi^{(p)}}(t, a) \right| \leq \varepsilon E_{W,k,r,p}^{[2]}(t, a), \quad (43)$$

with $E_{W,k,r,p}^{[2]}(t, a) = a^{r+1} M J_{r+1,p} + (\frac{\pi}{3} a^{r+3} M J_{r+3,p} + K_{W,r,p}) A_k(t)$. Consequently, for any $(t, a) \in Z_k$:

$$\left| W_f^{t^r \psi^{(p)}}(t, a) - W_{f_k}^{t^r \psi^{(p)}}(t, a) \right| \leq \varepsilon \sum_{l \neq k} E_{W,l,r,p}^{[2]}(t, a) := \varepsilon \Omega_{W,k,r,p}^{[2]}(t, a). \quad (44)$$

Furthermore, for any $k \in \{1, \dots, K\}$, any $r \in \{0, 1\}$ and $p \in \{0, 1\}$, and $(t, a) \in \mathbb{R} \times \mathbb{R}_+$, one has:

$$\left| W_{f_k}^{t^r \psi^{(p)}}(t, a) - W_{f_{k,1}}^{t^r \psi^{(p)}}(t, a) \right| \leq \varepsilon \Gamma_{W,k,r,p}^{[2]}(t, a), \quad (45)$$

where $W_{f_{k,1}}^{t^r \psi^{(p)}}(t, a) = f_k(t) \mathcal{F}\{\tau^r \psi^{(p)}(\tau) e^{i\pi \phi''(t) a^2 \tau^2}\} (a \phi'(t))^*$ and $\Gamma_{W,k,r,p}^{[2]}(t, a) = a^{r+1} M J_{r+1,p} + \frac{\pi}{3} a^{r+3} M J_{r+3,p} A_k(t)$.

Proof. Following the same steps as the proof of Proposition 1, but using a zeroth order Taylor expansion of the amplitude and second order expansion of the phase of f_k , one has:

$$\begin{aligned} f_k(\tau) &= A_k(\tau) e^{i2\pi \phi_k(\tau)} \\ &= A_k(t) e^{i2\pi[\phi_k(t) + \phi'_k(t)(\tau-t) + \frac{1}{2}\phi''_k(t)(\tau-t)^2]} + (A_k(\tau) - A_k(t)) e^{i2\pi \phi_k(\tau)} \\ &\quad + A_k(t) \left[e^{i2\pi[\phi_k(t) + \phi'_k(t)(\tau-t) + \frac{1}{2}\phi''_k(t)(\tau-t)^2 + \frac{1}{2} \int_t^\tau \phi''_k(x)(\tau-x)^2 dx]} \right. \\ &\quad \left. - e^{i2\pi[\phi_k(t) + \phi'_k(t)(\tau-t) + \frac{1}{2}\phi''_k(t)(\tau-t)^2]} \right] \\ &= f_{k,1}(\tau) + f_{k,2}(\tau) + f_{k,3}(\tau). \end{aligned}$$

Then, for any $(t, a) \in \mathbb{R} \times \mathbb{R}_+$,

$$\begin{aligned} W_{f_{k,1}}^{t^r \psi^{(p)}}(t, a) &= \frac{f_k(t)}{a} \int_{\mathbb{R}} e^{i\pi \phi_k''(t)(\tau-t)^2} \left(\frac{\tau-t}{a} \right)^r \psi^{(p)} \left(\frac{\tau-t}{a} \right)^* e^{i2\pi \phi_k'(t)(\tau-t)} d\tau \\ &= f_k(t) \mathcal{F}\{\tau^r \psi^{(p)}(\tau) e^{i\pi \phi_k''(t)a^2\tau^2}\} (a\phi_k'(t))^*, \\ \left| W_{f_{k,2}}^{t^r \psi^{(p)}}(t, a) \right| &\leq \frac{1}{a} \int_{\mathbb{R}} |A_k(\tau) - A_k(t)| |\tau - t|^r \left| \psi^{(p)} \left(\frac{\tau-t}{a} \right) \right| d\tau \\ &= \varepsilon a^{r+1} M J_{r+1,p}, \end{aligned}$$

and

$$\begin{aligned} |W_{f_{k,3}}^{t^r \psi^{(p)}}(t, a)| &\leq \frac{\pi A_k(t)}{a} \int_{\mathbb{R}} \left(\int_t^\tau |\phi'''(x)| |\tau - x|^2 dx \right) |\tau - t|^r \left| \psi^{(p)} \left(\frac{\tau-t}{a} \right) \right| d\tau \\ &= \varepsilon \frac{\pi}{3} a^{r+3} M A_k(t) J_{r+3,p}. \end{aligned}$$

For $(t, a) \notin Z_k$, the assumptions on ψ lead to $|W_{f_{k,1}}^{t^r \psi^{(p)}}(t, a)| \leq \varepsilon K_{W,r,p} A_k(t)$. As a result, one gets the inequalities (43) and (44). Also, for $(t, a) \in \mathbb{R} \times \mathbb{R}_+$, one easily get (45). \square

(a) Now, if $(t, a) \in \mathbb{E} \setminus \bigcup_{l=1}^K Z_l$, we immediately get:

$$|W_f^\psi(t, a)| \leq \varepsilon \sum_{l=1}^K E_{W,l,0,0}^{[2]}(t, a) \leq \tilde{\varepsilon},$$

when $\tilde{\varepsilon}$ is sufficiently small, which proves item (a) of Theorem 2. Indeed, one can find $\tilde{\varepsilon}$ such that:

$$\tilde{\varepsilon} \leq \left\| \sum_{l=1}^K E_{W,l,0,0}^{[2]}(t, a) \right\|_{\infty, \mathbb{E} \setminus \bigcup_{l=1}^K Z_l}^{-\frac{1}{2}}, \quad (46)$$

because $E_{W,l,0,0}^{[2]}(t, a)$ is bounded on $\mathbb{E} \setminus \bigcup_{l=1}^K Z_l$.

Now, we introduce the following propositions that are useful to prove item (b) of Theorem 2.

Proposition 8. For $(t, a) \in Z_k$ and $p \in \{0, 1\}$, assuming ψ satisfies the hypotheses of Theorem 2, one has:

$$\left| W_f^{\psi(p+1)}(t, a) + i2\pi a \left(\phi'_k(t) W_f^{\psi(p)}(t, a) + a\phi''_k(t) W_f^{t\psi(p)}(t, a) \right) \right| \leq \varepsilon B_{W,k,p}^{[2]}(t, a), \quad (47)$$

where

$$\begin{aligned} B_{W,k,p}^{[2]}(t, a) = & aMKJ_{0,p} + \pi a^3 M J_{2,p} \sum_{k=1}^K \|A_k\|_\infty \\ & + 2\pi a \sum_{l \neq k} \left(\phi'_l(t) E_{W,l,0,p}^{[2]}(t, a) + |\phi''_l(t)| E_{W,l,1,p}^{[2]}(t, a) \right) \\ & + 2\pi a \left(\phi'_k(t) \Omega_{W,k,0,p}^{[2]}(t, a) + |\phi''_k(t)| \Omega_{W,k,1,p}^{[2]}(t, a) \right). \end{aligned}$$

Proof. Doing the same thing as the proof of Proposition 2, but using a zeroth order Taylor expansion of the amplitude and second order expansion of the phase of f_k , one has:

$$\begin{aligned} \partial_t W_f^{\psi(p)}(t, a) = & \frac{1}{a} \sum_{k=1}^K \int_{\mathbb{R}} A'_k(\tau) e^{i2\pi\phi_k(\tau)} \psi^{(p)} \left(\frac{\tau - t}{a} \right)^* d\tau \\ & + i2\pi \sum_{k=1}^K \phi'_k(t) W_{f_k}^{\psi(p)}(t, a) + i2\pi a \sum_{k=1}^K \phi''_k(t) W_{f_k}^{t\psi(p)}(t, a) \\ & + \frac{1}{a} \sum_{k=1}^K \int_{\mathbb{R}} A_k(\tau) i2\pi \left(\int_t^\tau (\tau - u) \phi_k'''(u) du \right) e^{i2\pi\phi_k(\tau)} \psi^{(p)} \left(\frac{\tau - t}{a} \right)^* d\tau. \end{aligned}$$

Note that since $\partial_t W_f^{\psi(p)}(t, a) = -\frac{1}{a} W_f^{\psi(p+1)}(t, a)$, one may then write:

$$\begin{aligned} & \left| W_f^{\psi(p+1)}(t, a) + i2\pi a \sum_{k=1}^K \left(\phi'_k(t) W_{f_k}^{\psi(p)}(t, a) + a\phi''_k(t) W_{f_k}^{t\psi(p)}(t, a) \right) \right| \\ & \leq \varepsilon \left(aMKJ_{0,p} + \pi a^3 M J_{2,p} \sum_{k=1}^K \|A_k\|_\infty \right). \end{aligned}$$

From Proposition 7, we first have, when $(t, a) \in Z_k$:

$$\begin{aligned} & \left| W_f^{\psi^{(p+1)}}(t, a) + i2\pi a \left(\phi'_k(t) W_{f_k}^{\psi^{(p)}}(t, a) + a\phi''_k(t) W_{f_k}^{t\psi^{(p)}}(t, a) \right) \right| \\ & \leq \varepsilon \left(aMKJ_{0,p} + \pi a^3 M J_{2,p} \sum_{k=1}^K \|A_k\|_\infty \right. \\ & \quad \left. + 2\pi a \sum_{l \neq k} \left(\phi'_l(t) E_{W,l,0,p}^{[2]}(t, a) + |\phi''_l(t)| E_{W,l,1,p}^{[2]}(t, a) \right) \right), \end{aligned}$$

and then,

$$\begin{aligned} & \left| W_f^{\psi^{(p+1)}}(t, a) + i2\pi a \left(\phi'_k(t) W_f^{\psi^{(p)}}(t, a) + a\phi''_k(t) W_f^{t\psi^{(p)}}(t, a) \right) \right| \\ & \leq \varepsilon \left(aMKJ_{0,p} + \pi a^3 M J_{2,p} \sum_{k=1}^K \|A_k\|_\infty \right. \\ & \quad + 2\pi a \sum_{l \neq k} \left(\phi'_l(t) E_{W,l,0,p}^{[2]}(t, a) + |\phi''_l(t)| E_{W,l,1,p}^{[2]}(t, a) \right) \\ & \quad \left. + 2\pi a (\phi'_k(t) \Omega_{W,k,0,p}^{[2]}(t, a) + |\phi''_k(t)| \Omega_{W,k,1,p}^{[2]}(t, a)) \right), \end{aligned}$$

which results in (47). \square

Proposition 9. *For any $(t, a) \in Z_k$ such that $|W_f^\psi(t, a)| > \tilde{\varepsilon}$ and $|\partial_t \tilde{\tau}_{W_f^\psi}(t, a)| > \tilde{\varepsilon}$ one has:*

$$|\tilde{q}_{t, W_f^\psi}(t, a) - \phi''_k(t)| \leq \tilde{\varepsilon}. \quad (48)$$

Proof.

$$\begin{aligned}
& |\phi_k''(t) - \tilde{q}_{t, W_f^\psi}(t, a)| \\
&= \left| \frac{1}{2\pi a^2} \frac{W_f^{\psi'} [W_f^{\psi'} + i2\pi a^2 \phi_k''(t) W_f^{t\psi}] - W_f^\psi [W_f^{\psi''} + i2\pi a^2 \phi_k''(t) W_f^{t\psi'}]}{W_f^{t\psi} W_f^{\psi'} - W_f^{t\psi'} W_f^\psi} \right| \\
&\leq \left| \frac{1}{2\pi a^2} \frac{W_f^{\psi'} [W_f^{\psi'} + i2\pi a (\phi_k'(t) W_f^\psi + a \phi_k''(t) W_f^{t\psi})]}{W_f^{t\psi} W_f^{\psi'} - W_f^{t\psi'} W_f^\psi} \right| \\
&\quad + \left| \frac{1}{2\pi a^2} \frac{W_f^\psi [W_f^{\psi''} + i2\pi a (\phi_k'(t) W_f^{\psi'} + a \phi_k''(t) W_f^{t\psi'})]}{W_f^{t\psi} W_f^{\psi'} - W_f^{t\psi'} W_f^\psi} \right| \\
&\leq \varepsilon B_{W,k,0}^{[2]}(t, a) \left| \frac{1}{2\pi a^2} \frac{W_f^{\psi'}}{W_f^{t\psi} W_f^{\psi'} - W_f^{t\psi'} W_f^\psi} \right| \\
&\quad + \varepsilon B_{W,k,1}^{[2]}(t, a) \left| \frac{1}{2\pi a^2} \frac{W_f^\psi}{W_f^{t\psi} W_f^{\psi'} - W_f^{t\psi'} W_f^\psi} \right| \\
&\leq \tilde{\varepsilon}^3 \left(\frac{B_{W,k,0}^{[2]}(t, a)}{2\pi a^2} |W_f^{\psi'}| + \frac{B_{W,k,1}^{[2]}(t, a)}{2\pi a^2} |W_f^\psi| \right) \leq \tilde{\varepsilon},
\end{aligned}$$

if $\tilde{\varepsilon}$ is sufficiently small, because $\frac{B_{W,k,0}^{[2]}(t, a)}{a^2}$, $\frac{B_{W,k,1}^{[2]}(t, a)}{a^2}$, $W_f^{\psi'}$ and W_f^ψ are all bounded on Z_k . \square

Now we can prove item (b) of Theorem 2.

(b) According to definition of $\tilde{\omega}_{t, W_f^\psi}^{[2]}(t, a)$ in (24), one has

$$\tilde{\omega}_{t, W_f^\psi}^{[2]}(t, a) = \tilde{\omega}_{W_f^\psi}(t, a) + \tilde{q}_{t, W_f^\psi}(t, a)(t - \tilde{\tau}_{W_f^\psi}(t, a)).$$

It follows that for $(t, a) \in Z_k$, such that $|W_f^\psi(t, a)| > \tilde{\varepsilon}$ and $|\partial_t \tilde{r}_{W_f^\psi}(t, a)| > \tilde{\varepsilon}$

$$\begin{aligned}
& \left| \tilde{\omega}_{t, W_f^\psi}^{[2]}(t, a) - \phi'_k(t) \right| \\
&= \left| \frac{1}{i2\pi a} \frac{W_f^{\psi'}(t, a) + i2\pi a \phi'_k(t) W_f^\psi(t, a) + i2\pi a^2 \phi''_k(t) W_f^{t\psi}(t, a)}{W_f^\psi(t, a)} \right| \\
&\quad + \left| a \frac{\left(\tilde{q}_{t, W_f^\psi}(t, a) - \phi''_k(t) \right) W_f^{t\psi}(t, a)}{W_f^\psi(t, a)} \right| \\
&\leq \varepsilon \frac{B_{W, k, 0}^{[2]}(t, a)}{|2\pi a W_f^\psi(t, a)|} + a \frac{|\tilde{q}_{t, W_f^\psi}(t, a) - \phi''_k(t)| |W_f^{t\psi}(t, a)|}{|W_f^\psi(t, a)|} \\
&\leq \varepsilon \frac{B_{W, k, 0}^{[2]}(t, a)}{|2\pi a W_f^\psi(t, a)|} \\
&\quad + a \tilde{\varepsilon}^3 \frac{|(B_{W, k, 0}^{[2]}(t, a) |W_f^{\psi'}| + B_{W, k, 1}^{[2]}(t, a) |W_f^\psi|) |W_f^{t\psi}(t, a)|}{|W_f^\psi(t, a)|} \leq \tilde{\varepsilon}
\end{aligned}$$

when $\tilde{\varepsilon}$ is sufficiently small.

(c) The proof of item (c) of Theorem 2 is exactly the same as in the weak modulation case, except that we use, at the very end of the proof, the hypothesis:

$$\left| \frac{1}{C'_\psi} \int_{\{\eta \text{ s.t. } |\eta-1| > \Delta\}} \mathcal{F}\{\psi(\tau) e^{-i\pi \phi''_l(t) a^2 \tau^2}\}(\eta)^* \frac{d\eta}{\eta} \right| \leq \frac{K_3 \tilde{\varepsilon}}{C'_\psi} \text{ for any } l,$$

and

$$\frac{1}{|C'_\psi|} \left| \int_{\{a \text{ s.t. } |a \phi'_k(t) - 1| < \Delta \text{ and } |W_f^\psi(t, a)| \leq \tilde{\varepsilon}\}} W_f^\psi(t, a) \frac{da}{a} \right| \leq \left| \frac{1}{C'_\psi} \right| \log \left(\frac{1 + \Delta}{1 - \Delta} \right) \tilde{\varepsilon}$$

to compute $D_W^{[2]}$:

$$\begin{aligned}
D_W^{[2]} = \frac{1}{|C'_\psi|} & \left[\left(\|\Omega_{W, k, r, p}^{[2]}(t, a)\|_{\infty, \bigcup_{l=1}^K Z_l} + \|\Gamma_{W, k, r, p}^{[2]}(t, a)\|_{\infty, \bigcup_{l=1}^K Z_l} + 1 \right) \log \left(\frac{1 + \Delta}{1 - \Delta} \right) \right. \\
& \left. + \max_k \|A_k\|_\infty K_3 \right],
\end{aligned}$$

which also finishes the proof.

References

- [1] I. Daubechies, J. Lu, and H.-T. Wu, “Synchrosqueezed wavelet transforms: an empirical mode decomposition-like tool,” *Applied and Computational Harmonic Analysis*, vol. 30, no. 2, pp. 243–261, 2011.
- [2] T. Oberlin and S. Meignen, “The second-order wavelet synchrosqueezing transform,” in *42th International Conference on Acoustics, Speech, and Signal Processing (ICASSP)*, 2017.
- [3] M. Costa, A. A. Priplata, L. A. Lipsitz, Z. Wu, N. E. Huang, A. L. Goldberger, and C.-K. Peng, “Noise and poise: Enhancement of postural complexity in the elderly with a stochastic-resonance-based therapy,” *Europhysics Letters (EPL)*, vol. 77, no. 6, p. 68008, Mar 2007.
- [4] D. A. Cummings, R. A. Irizarry, N. E. Huang, T. P. Endy, A. Nisalak, K. Ungchusak, and D. S. Burke, “Travelling waves in the occurrence of dengue haemorrhagic fever in Thailand,” *Nature*, vol. 427, no. 6972, pp. 344–347, Jan 2004.
- [5] N. E. Huang and Z. Wu, “A review on Hilbert-huang transform: Method and its applications to geophysical studies,” *Reviews of Geophysics*, vol. 46, no. 2, Jun 2008.
- [6] Y. Y. Lin, H.-T. Wu, C. A. Hsu, P. C. Huang, Y. H. Huang, and Y. L. Lo, “Sleep apnea detection based on thoracic and abdominal movement signals of wearable piezo-electric bands,” *IEEE Journal of Biomedical and Health Informatics*, 2016.
- [7] C. L. Herry, M. Frasch, A. J. Seely, and H.-T. Wu, “Heart beat classification from single-lead ecg using the synchrosqueezing transform,” *Physiological Measurement*, vol. 38, no. 2, pp. 171–187, 2017.
- [8] S. Meignen, T. Oberlin, and S. McLaughlin, “A new algorithm for multicomponent signals analysis based on synchrosqueezing: With an application to signal sampling and denoising,” *IEEE Transactions on Signal Processing*, vol. 60, no. 11, pp. 5787–5798, 2012.
- [9] P. Flandrin, *Time-frequency/time-scale analysis*. Academic Press, 1998, vol. 10.

- [10] K. Kodera, R. Gendrin, and C. Villedary, “Analysis of time-varying signals with small bt values,” *IEEE Transactions on Acoustics, Speech, and Signal Processing*, vol. 26, no. 1, pp. 64–76, Feb 1978.
- [11] F. Auger and P. Flandrin, “Improving the readability of time-frequency and time-scale representations by the reassignment method,” *IEEE Transactions on Signal Processing*, vol. 43, no. 5, pp. 1068–1089, 1995.
- [12] G. Thakur and H.-T. Wu, “Synchrosqueezing-based recovery of instantaneous frequency from nonuniform samples,” *SIAM J. Math. Analysis*, vol. 43, no. 5, pp. 2078–2095, 2011.
- [13] M. Clausel, T. Oberlin, and V. Perrier, “The monogenic synchrosqueezed wavelet transform: a tool for the decomposition/demodulation of am-fm images,” *Applied and Computational Harmonic Analysis*, vol. 39, no. 3, pp. 450–486, Nov 2015.
- [14] H. Yang, “Synchrosqueezed wave packet transforms and diffeomorphism based spectral analysis for 1d general mode decompositions,” *Applied and Computational Harmonic Analysis*, vol. 39, no. 1, pp. 33–66, July 2015.
- [15] H. Yang and L. Ying, “Synchrosqueezed wave packet transform for 2D mode decomposition,” *SIAM Journal on Imaging Sciences*, vol. 6, no. 4, pp. 1979–2009, Jan 2013.
- [16] I. Daubechies, Y. G. Wang, and H.-T. Wu, “Conceft: concentration of frequency and time via a multitapered synchrosqueezed transform,” *Philosophical Transactions of the Royal Society A: Mathematical, Physical and Engineering Sciences*, vol. 374, no. 2065, Mar 2016.
- [17] M. Skolnik, *Radar Handbook*, Technology and Engineering, Eds. McGraw-Hill Education, 2008.
- [18] J. W. Pitton, L. E. Atlas, and P. J. Loughlin, “Applications of positive time-frequency distributions to speech processing,” *IEEE Transactions on Speech and Audio Processing*, vol. 2, no. 4, pp. 554–566, 1994.
- [19] E. J. Candes, P. R. Charlton, and H. Helgason, “Detecting highly oscillatory signals by chirplet path pursuit,” *Applied and Computational Harmonic Analysis*, vol. 24, no. 1, pp. 14–40, 2008.

- [20] B. P. Abbott and al., “Observation of gravitational waves from a binary black hole merger,” *Phys. Rev. Lett.*, vol. 116, 2016.
- [21] T. Oberlin, S. Meignen, and V. Perrier, “The fourier-based synchrosqueezing transform,” in *2014 IEEE International Conference on Acoustics, Speech and Signal Processing (ICASSP)*, May 2014, pp. 315–319.
- [22] R. Behera, S. Meignen, and T. Oberlin, “Theoretical analysis of the second-order synchrosqueezing transform,” *Applied and Computational Harmonic Analysis*, Nov 2016.
- [23] I. Daubechies and S. Maes, “A nonlinear squeezing of the continuous wavelet transform based on auditory nerve models,” *Wavelets in medicine and biology*, pp. 527–546, 1996.
- [24] H.-T. Wu, “Adaptive analysis of complex data sets,” Ph.D. dissertation, Princeton, 2011.
- [25] F. Auger, P. Flandrin, Y.-T. Lin, S. McLaughlin, S. Meignen, T. Oberlin, and H.-T. Wu, “Time-frequency reassignment and synchrosqueezing: An overview,” *IEEE Signal Processing Magazine*, vol. 30, no. 6, pp. 32–41, 2013.
- [26] T. Oberlin, S. Meignen, and V. Perrier, “Second-order synchrosqueezing transform or invertible reassignment? Towards ideal time-frequency representations,” *IEEE Transactions on Signal Processing*, vol. 63, no. 5, pp. 1335–1344, March 2015.
- [27] D.-H. Pham and S. Meignen, “High-order synchrosqueezing transform for multicomponent signals analysis - with an application to gravitational-wave signal,” *IEEE Transactions on Signal Processing*, vol. 65, no. 12, pp. 3168–3178, June 2017.
- [28] S. Mallat, *A Wavelet Tour of Signal Processing, Third Edition: The Sparse Way*, 3rd ed. Academic Press, 2008.
- [29] R. Carmona, W. Hwang, and B. Torresani, “Characterization of signals by the ridges of their wavelet transforms,” *IEEE Transactions on Signal Processing*, vol. 45, no. 10, pp. 2586–2590, Oct 1997.

- [30] G. Thakur, E. Brevdo, N. S. FućKar, and H.-T. Wu, “The synchrosqueezing algorithm for time-varying spectral analysis: Robustness properties and new paleoclimate applications,” *Signal Processing*, vol. 93, no. 5, pp. 1079–1094, May 2013.
- [31] H. Yang, “Statistical analysis of synchrosqueezed transforms,” *Applied and Computational Harmonic Analysis*, Jan. 2017.